

Large Magnetic Entropy Change in $\text{La}_{0.6}\text{Ce}_{0.4}\text{Fe}_{11.5}\text{Si}_{1.5}$ Alloy Exhibiting First- and Second-Order Phase Transitions

Tran Dang Thanh¹, W. Z. Nan², B. Y. Jeon³, T. S. Yu³, Jong Suk Lee⁴, Hoang Nam Nhat⁵, and Seong Cho Yu²

¹*Institute of Materials Science, Vietnam Academy of Science and Technology, 18-Hoang Quoc Viet Hanoi, Vietnam*

²*Department of Physics, Chungbuk National University, Cheongju 361-763, Korea*

³*Department of Chemistry, Chungbuk National University, Cheongju 361-763, Korea*

⁴*Department of Mechanical Engineering, Gangneung-Wonju National University, Gangwon 210-702, Korea*

⁵*Faculty of Engineering Physics and Nanotechnology, VNU-University of Engineering and Technology, 144 Xuan Thuy, Ha Noi, Viet Nam*

Received 29 Oct 2015, revised 26 Nov 2015, accepted 8 Dec 2015, published 17 Dec 2015, current version 22 Feb 2016.

Abstract—A polycrystalline alloy ingot of $\text{La}_{0.6}\text{Ce}_{0.4}\text{Fe}_{11.5}\text{Si}_{1.5}$ was prepared by an arc-melting method. Magnetic measurements of magnetization M as a function of field H and temperature T show a ferromagnetic–paramagnetic phase transition at a Curie temperature $T_C = 170$ K. Interestingly, curves of H/M versus M^2 have a positive slope at low field ($H \leq 10$ kOe), which corresponds to a second-order phase transition (SOPT), but a negative slope at high field ($H > 10$ kOe), which corresponds to a first-order phase transition (FOPT). The magnetic entropy change $\Delta S_m(T)$ under different ranges of field change ΔH , calculated from $M(H)$ isotherms, has a maximum $|\Delta S_{\max}|$ around T_C that increases in magnitude with increasing ΔH . Refrigerant capacity (RC), indicative of magnetic cooling efficiency, also increases with increasing ΔH . Curves of $\Delta S_m(T)/\Delta S_{\max}$ versus $\theta = (T - T_C)/(T_r - T_C)$, where T_r is the reference temperature, collapse into a universal curve when $\Delta H \leq 10$ kOe. In contrast, curves of $\Delta S_m(T)/\Delta S_{\max}$ versus θ do not reduce to a universal curve when $\Delta H > 10$ kOe. These suggest a coexistence of FOPT and SOPT properties in the alloy.

Index Terms—Magnetism in solids, electromagnetics, soft magnetic materials, magnetic instruments.

I. INTRODUCTION

The magnetocaloric effect (MCE) is heating or cooling of a magnetic material under the change of external magnetic field. Physical quantity describing MCE is adiabatic temperature change. The MCE exhibited is usually maximized when the material is near the magnetic ordering temperature. This is related to a magnetic entropy change (ΔS_m) under the application of an external magnetic field. Recently, the MCE has attracted the attention of researchers and can be referenced in a large number of publications. The reviews in the MCE were made by Gschneider [2005] and recently rather extensively by Phan and Yu [2007] and Franco [2012]. Magnetic refrigeration based on the MCE is currently a promising technology, which can replace the conventional technology based on gaseous compression/expansion cycles [Tishin 2003, Gschneider 2008]. It is appreciated because it is more efficient, inexpensive, and environmentally friendly. So far, Gd metal has been used as a prototypical refrigerant for room-temperature magnetic cooling because it has a Curie temperature $T_C = 294$ K and an MCE [Gschneider 2005, Wang 2005] with a maximum value of ΔS_m , $|\Delta S_{\max}| = 10.2 \text{ J kg}^{-1} \text{ K}^{-1}$ under an applied magnetic field change $\Delta H = 50$ kOe [Gschneider 2005]. Experimental results obtained from Gd-related alloys (such as Gd-Si-Ge, Gd-Co, etc.) [Pecharsky 1997, Provenzano 2004] have indicated a bright scenario of the magnetic refrigeration technology. However, Gd-containing alloys usually have very high costs due to the scarcity of raw materials along with a strict manufacturing technology. Many magnetocaloric materials [Gschneider 2005, Phan 2007, Franco 2012], including As-based alloys, Heusler alloys, $\text{La}(\text{Fe}, \text{Si})_{13}$ -type

alloys, and as well as perovskite manganites have been investigated for magnetic refrigeration applications. It has been also reported that materials undergoing a first-order phase transition (FOPT) show giant MCE with a large ΔS_m value, e.g., Ni-Mn-In alloys with $|\Delta S_{\max}| = 35\text{--}40 \text{ J} \cdot \text{kg}^{-1} \cdot \text{K}^{-1}$ at $\Delta H = 50$ kOe [Pathak 2007, Dubenko 2009], and Ni-Mn-Ga-based alloys with $|\Delta S_{\max}| = 40\text{--}60 \text{ J} \cdot \text{kg}^{-1} \cdot \text{K}^{-1}$ at $\Delta H = 50$ kOe [Dubenko 2009]. However, this MCE only occurs in a narrow temperature range. In contrast, materials with a second-order phase transition (SOPT) offer moderate ΔS_m values, but these ΔS_m values are stable over a wide temperature range so their refrigerant capacity (RC) values can be larger than those of FOPT materials. With such features, it is essential to investigate the influence of phase transformations on the MCE. Additionally, detailed analyses for $\Delta S_m(T, \Delta H)$ data would provide important information about magnetic properties of materials [Chandra 2012]. To get a clear idea about the performance of materials used in magnetic refrigeration devices, it is necessary to understand how their MCE evolves in desired temperature and magnetic-field ranges.

In this work, we present a coexistence of FOPT and SOPT properties with the large $|\Delta S_{\max}|$ and RC values in the $\text{La}_{0.6}\text{Ce}_{0.4}\text{Fe}_{11.5}\text{Si}_{1.5}$ alloy. We point out that the $\text{La}_{0.6}\text{Ce}_{0.4}\text{Fe}_{11.5}\text{Si}_{1.5}$ alloy undergoes SOPT under low-field ($\Delta H \leq 10$ kOe), whereas it exhibits characters of a FOPT material under high-field ($\Delta H = 10\text{--}30$ kOe).

II. EXPERIMENT

An alloy ingot sample with a composition of $\text{La}_{0.6}\text{Ce}_{0.4}\text{Fe}_{11.5}\text{Si}_{1.5}$ was prepared from La, Ce, Fe, and Si metals (3N purity) by an arc-melting method in an Ar ambience. After that, the alloy was sealed in a quartz tube and annealed at 1323 K for 48 h. in an Ar ambience. The crystal structure of the sample at room temperature

Corresponding author: S. C. Yu (scyu@chungbuk.ac.kr). Donostia International Workshop on Energy, Materials, and Nanotechnology, San Sebastian, Spain, 1–4 September 2015.

Digital Object Identifier 10.1109/LMAG.2015.2509943

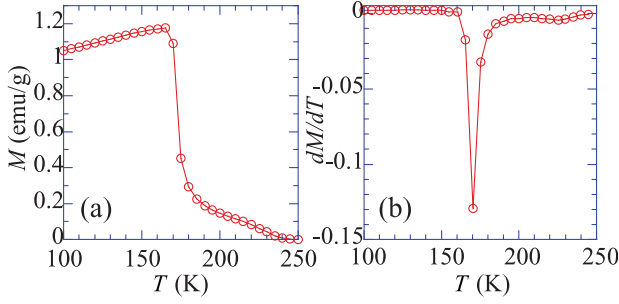


Fig. 1. (a) $M_{ZFC}(T)$ and its (b) dM/dT versus T curves for $\text{La}_{0.6}\text{Ce}_{0.4}\text{Fe}_{11.5}\text{Si}_{1.5}$ alloy under an applied magnetic field 30 Oe.

was checked by using on X-ray diffractometer (Bruker AXS, D8 Discover), used a $\text{Cu} - K\alpha$ radiation source ($\lambda = 1.5406 \text{ \AA}$). X-ray diffraction pattern (not shown) indicates that sample is single phase $\text{La}_{0.6}\text{Ce}_{0.4}\text{Fe}_{11.5}\text{Si}_{1.5}$ in the cubic NaZn_{13} -type structure with a space group of $\text{Fm}\bar{3}\text{c}$, without any trace of secondary phases. Based on the XRD data, the lattice parameters for alloy were calculated, $a = 11.456 \text{ \AA}$ and $V = 1503.485 \text{ \AA}^3$. The magnetization measurements versus temperature ($T = 50\text{--}350 \text{ K}$) and magnetic field ($H = 0\text{--}30 \text{ kOe}$) were performed on a vibrating sample magnetometer (VersaLab—Quantum design) using a warming mode. Here, the temperature interval between magnetic field isotherms was 2 K near the phase transition temperatures.

III. RESULTS AND DISCUSSION

Fig. 1 shows temperature dependence of zero-field-cooled (ZFC) $M_{ZFC}(T)$, and its dM/dT curves for $\text{La}_{0.6}\text{Ce}_{0.4}\text{Fe}_{11.5}\text{Si}_{1.5}$ alloy under an applied magnetic field of 30 Oe. It appears that the sample exhibits a ferromagnetic (FM)–paramagnetic (PM) phase transition at around 170 K. By performing dM/dT versus T curve, the T_C value of this sample is found to be 170 K. However, there is a small hump at temperature above 200 K. This suggests that the sample is magnetically inhomogeneous. To further understand the magnetic property and the phase transition type in the sample, we have recorded isothermal magnetization $M(H)$ curves at various temperatures in a range of 140–200 K with increasing step of 2 K. Fig. 2(a) shows $M(H)$ curves for $\text{La}_{0.6}\text{Ce}_{0.4}\text{Fe}_{11.5}\text{Si}_{1.5}$ alloy at several representative temperatures around the FM–PM phase transition. The magnetization increases most abruptly in weak applied field ($H < 3 \text{ kOe}$) and then approaches to saturation for above 4 kOe. At a given H , the magnetization value decreases with increasing temperature. However, at temperatures ranging from 164 to 180 K, besides a decrease in magnetization with increasing temperature, a sudden change in slope of the $M(H)$ curves at high-field can be observed. This suggests an existence of magnetical inhomogeneity and/or the additional presence of anti-FM interactions.

To assess the nature of the phase transitions, H/M versus M^2 curves were constructed; see Fig. 2(b). According to Banerjee's [1964] criteria, the slope of H/M versus M^2 curves indicates the nature of the FM–PM transition: if some of the H/M versus M^2 curves show a negative slope at some points, the transition is of the FOPT, whereas a positive slope corresponds to the SOPT. Clearly, the H/M versus M^2 curves at low field ($H \leq 10 \text{ kOe}$) exhibit a positive

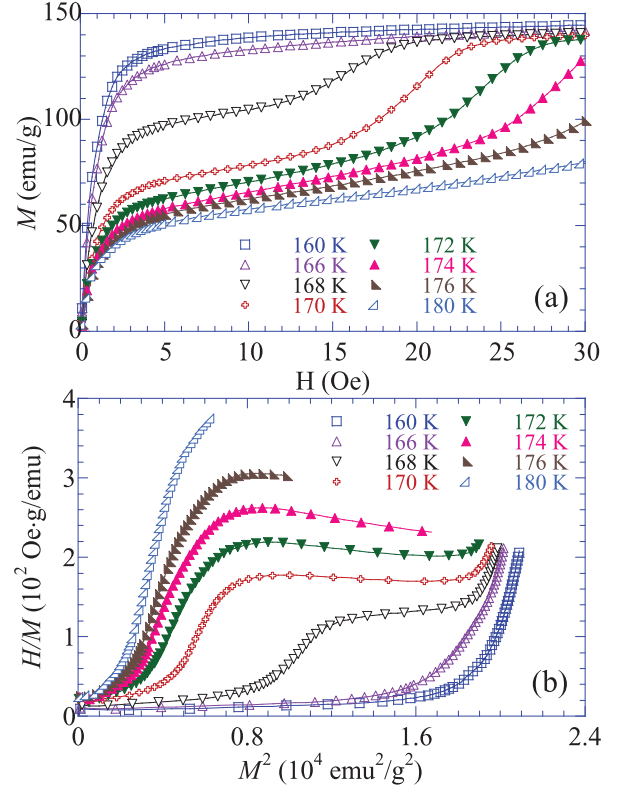


Fig. 2. (a) $M(H)$ and (b) H/M versus M^2 curves at some representative temperatures around T_C for $\text{La}_{0.6}\text{Ce}_{0.4}\text{Fe}_{11.5}\text{Si}_{1.5}$ alloy.

slope, corresponding to the SOPT, whereas a negative slope corresponding to the FOPT was observed at high field ($H > 10 \text{ kOe}$). This indicates that a coexistence of FOPT and SOPT properties in $\text{La}_{0.6}\text{Ce}_{0.4}\text{Fe}_{11.5}\text{Si}_{1.5}$ alloy.

Based on the $M(H)$ data above, the MCE of $\text{La}_{0.6}\text{Ce}_{0.4}\text{Fe}_{11.5}\text{Si}_{1.5}$ alloy can be assessed upon the ΔS_m calculated from the Maxwell relation as follows:

$$\Delta S_m(T, \Delta H) = \int_0^{H_{\max}} \left(\frac{\partial M(T, H)}{\partial T} \right)_H dH \quad (1)$$

where $\Delta H = H_{\max}$ is an applied magnetic field change. Fig. 3(a) shows $\Delta S_m(T)$ curves for magnetic-field changes $\Delta H = 5\text{--}30 \text{ kOe}$ with step of 5 kOe. As a function of temperature, $\Delta S_m(T)$ curves reach a maximum value at around the FM–PM phase transition. The absolute values of ΔS_m increase gradually with increasing ΔH . With $\Delta H = 10, 20, \text{ and } 30 \text{ kOe}$, $|\Delta S_{\max}|$ values are found to be 13.2, 26.0, and $33.2 \text{ J} \cdot \text{kg}^{-1} \cdot \text{K}^{-1}$, respectively, as shown in Table 1, indicating a giant MCE. The values of $|\Delta S_{\max}|$ for $\text{La}_{0.6}\text{Ce}_{0.4}\text{Fe}_{11.5}\text{Si}_{1.5}$ alloy are also plotted as a function of ΔH in Fig. 3(b). These values are higher than those obtained from other $\text{La}(\text{Fe, Si})_{13}$ -type alloys reported [Hu 2001, Jia 2009, Chen 2014, Boutahar 2014]. Together with $|\Delta S_{\max}|$, there is another useful parameter to assess the MCE of a magnetic material, which is refrigerant capacity (RC) defined as [Wood 1985]

$$\text{RC}(\delta T, H_{\max}) = \int_{T_{\text{cold}}}^{T_{\text{hot}}} \Delta S_m(T, H_{\max}) dT \quad (2)$$

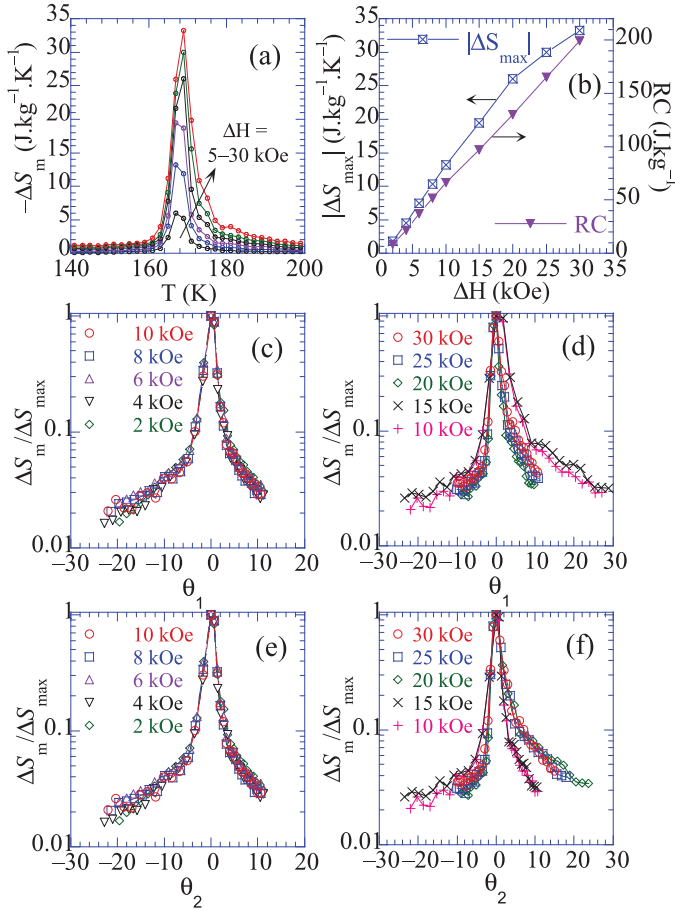


Fig. 3. (a) $\Delta S_m(T)$ under $\Delta H = 5\text{--}30$ kOe (with step 5 kOe). (b) $|\Delta S_{\max}|$ and RC versus ΔH . (c) and (d) $\Delta S_m(T)/\Delta S_{\max}$ versus θ_1 curves. (e) and (f) $\Delta S_m(T)/\Delta S_{\max}$ versus θ_2 curves in log-log scale.

where $\delta T = T_{\text{hot}} - T_{\text{cold}}$, with T_{cold} and T_{hot} viewed as corresponding to their full width at half maximum of the $-\Delta S_m(T)$ curve. Depending on ΔH , the RC value is found to be 66.0, 130.0, and 199.2 J kg^{-1} for $\Delta H = 10, 20$, and 30 kOe, respectively, as shown in Fig. 3(b) and Table 1. For a comparison, Table 1 also shows the $|\Delta S_{\max}|$ and RC values of Gd [Gschneidner 2005, Wang 2005] and La(Fe, Si)₁₃-type alloys reported in recent publications [Hu 2001, Jia 2009, Chen 2014, Boutahar 2014]. To compare the magnitude of the MCE of different magnetic materials and under different applied magnetic field change, the ratios of $|\Delta S_{\max}|/\Delta H$ and $\text{RC}/\Delta H$ could be used. In our case, the ratio of $|\Delta S_{\max}|/\Delta H = 1.1\text{--}1.3 \text{ J} \cdot \text{kg}^{-1} \cdot \text{K}^{-1} \cdot \text{kOe}^{-1}$ obtained for La_{0.6}Ce_{0.4}Fe_{11.5}Si_{1.5} alloy is higher than those obtained from other La(Fe, Si)₁₃-type alloys, such as LaFe_{13-x}Si_x [Hu 2001, Jia 2009, Chen 2014, Boutahar 2014] and La_{0.8}Ce_{0.2}Fe_{11.7}Si_{1.3} [Jia 2009], as well as Gd [Gschneidner 2005, Wang 2005]. However, the ratio of $\text{RC}/\Delta H = 6.6$ obtained for La_{0.6}Ce_{0.4}Fe_{11.5}Si_{1.5} alloy is very close to those obtained for other La(Fe, Si)₁₃-type alloys [Hu 2001, Jia 2009, Chen 2014, Boutahar 2014].

More recently, a new criterion for determining the nature of a transition has been proposed by Franco and Conde [2010] upon the rescaling of entropy change curves. Universal behavior manifested in the collapse of $\Delta S_m(T)$ data points measured under different ΔH values after a scaling procedure has been established for SOPT

Table 1. Experimental values for La_{0.6}Ce_{0.4}Fe_{11.5}Si_{1.5} alloy compared to those of Gd and some La(Fe, Si)₁₃-type alloys.

Material	ΔH (kOe)	$ \Delta S_{\max} $ (J/kg.K)	$ \Delta S_{\max} /\Delta H$ (J/kg.K.kOe)	RC (J/kg)	RC/ ΔH (J/kg.kOe)	Ref.
La _{0.6} Ce _{0.4} Fe _{11.5} Si _{1.5}	10	13.2	1.32	66.0	6.60	This work
La _{0.6} Ce _{0.4} Fe _{11.5} Si _{1.5}	20	26.0	1.30	130.0	6.50	
La _{0.6} Ce _{0.4} Fe _{11.5} Si _{1.5}	30	33.2	1.11	199.2	6.64	
Gd	10	2.8	0.280	63.4	6.34	[Wang 2005]
Gd	50	10.2	0.204	410	8.20	[Gschneidner 2005]
LaFe _{11.4} Si _{1.6}	10	10.5	1.05	-	-	[Hu 2001]
LaFe _{11.4} Si _{1.6}	20	14.3	0.715	-	-	
LaFe _{11.4} Si _{1.6}	50	19.4	0.388	-	-	[Jia 2009]
LaFe _{11.7} Si _{1.3}	50	29	0.580	-	-	
La _{0.8} Ce _{0.2} Fe _{11.7} Si _{1.3}	50	29	0.580	-	-	[Chen 2014]
LaFe _{11.5} Si _{1.5}	20	14.9-17.7	0.745-0.885	138.8-144.2	6.94-7.21	[Boutahar 2014]
LaFe _{11.8} Si _{1.2}	20	11	0.550	106.4	5.32	
LaFe _{11.6} Si _{1.4}	20	24.4	1.22	124	6.20	
LaFe _{11.5} Si _{1.5}	20	17.3	0.865	128	6.40	
LaFe _{11.4} Si _{1.6}	20	16.5	0.825	155	7.75	
LaFe _{11.2} Si _{1.8}	20	6.5	0.325	142	7.10	
LaFe _{11.0} Si _{2.0}	20	3.8	0.190	125	6.25	
LaFe _{10.8} Si _{2.2}	20	2.3	0.115	137.7	6.88	

materials. In contrast, when applied to an FOPT material, this behavior is broken down [Franco 2010]. This criterion of $\Delta S_m(T)$ data has been confirmed in several magnetocaloric materials as an additional method to confirm the FM-PM phase transition in the materials undergoing either FOPT or SOPT [Bonilla 2010]. According to entropy scaling method, if a material exhibits a single magnetic phase transition, all $\Delta S_m(T)$ data measured under different ΔH values are constructed by plotting $\Delta S_m(T)/\Delta S_{\max}$ versus θ , where θ is the temperature variable defined by

$$\theta_1 = (T - T_C)/(T_r - T_C) \quad (3)$$

where T_r is the reference temperature corresponding to a certain fraction f that fulfills $\Delta S_m(T_r)/\Delta S_{\max} = f$. However, if a material consists of multiple phase transitions, two reference temperatures T_{r1} and T_{r2} are selected for each of the curves (one below and the other above T_C), and the temperature axis is rescaled as

$$\theta_2 = \begin{cases} -(T - T_C)/(T_{r1} - T_C), & T \leq T_C \\ (T - T_C)/(T_{r2} - T_C), & T > T_C. \end{cases} \quad (4)$$

The choice of f , and using either T_C or T_P (temperature at the peak of the $\Delta S_m(T)$ curve) in (3) and (4) do not affect the actual construction of the universal curve [Franco 2010, Bonilla 2010]. However, a combination of the Banerjee [1964] criteria and the universal curve method [Franco 2010] to assess the order of a magnetic-phase transformation will be more accurate. In this work, we identified T_C as the value of T_P and selected $f = 0.6$ when constructing the universal curve for La_{0.6}Ce_{0.4}Fe_{11.5}Si_{1.5} alloy at several values of $\Delta H = 2\text{--}10$ kOe with step of 2 kOe and $\Delta H = 10\text{--}30$ kOe with step of 5 kOe. Fig. 3(c)–(f) shows the normalized magnetic entropy change versus the rescaled temperature θ_1 and θ_2 . Clearly, all the $\Delta S_m(T)$ data points measured under low-applied magnetic-field change ($\Delta H = 2\text{--}10$ kOe) are collapsed into a unique curve in the whole temperature range in both case of the

rescaled temperature θ_1 and θ_2 . On the contrary, the $\Delta S_m(T)$ data do not follow a universal curve for the magnetic entropy change under high-applied magnetic-field change ($\Delta H = 10\text{--}30$ kOe). These features once again demonstrate the coexistence of SOPT at low-field and FOPT at high field as mentioned above.

IV. CONCLUSION

We have presented detailed analyses on temperature and magnetic-field dependences of ΔS_m for a $\text{La}_{0.6}\text{Ce}_{0.4}\text{Fe}_{11.5}\text{Si}_{1.5}$ alloy. Experimental results demonstrated the coexistence of SOPT at low field and FOPT at high field in the sample. The value of $|\Delta S_{\text{max}}|$ in the $-\Delta S_m(T)$ curves has been observed, which corresponds to FM-PM phase transition. With $\Delta H = 10\text{--}30$ kOe, $|\Delta S_{\text{max}}|$ values are found to be $13.2\text{--}33.2 \text{ J} \cdot \text{kg}^{-1} \cdot \text{K}^{-1}$, corresponding to $\text{RC} = 66.0\text{--}199.2 \text{ J} \cdot \text{kg}^{-1}$. These values are compared with those of some $\text{La}(\text{Fe}, \text{Si})_{13}$ -type alloys. However, the ratio of $|\Delta S_{\text{max}}|/\Delta H = 1.1\text{--}1.3 \text{ J} \cdot \text{kg}^{-1} \cdot \text{K}^{-1} \cdot \text{kOe}^{-1}$ obtained for $\text{La}_{0.6}\text{Ce}_{0.4}\text{Fe}_{11.5}\text{Si}_{1.5}$ alloy is higher than those for other $\text{La}(\text{Fe}, \text{Si})_{13}$ -type alloys. Additionally, the universal curves of all $\Delta S_m(T)$ data points measured with different ΔH values were constructed by plotting $\Delta S_m(T)/\Delta S_{\text{max}}$ versus θ_1 and θ_2 . We pointed out that the $\Delta S_m(T)$ data can be collapsed into a unique curve under low field. However, they do not follow a universal curve under high field. These features prove a large magnetic entropy change in $\text{La}_{0.6}\text{Ce}_{0.4}\text{Fe}_{11.5}\text{Si}_{1.5}$ alloy exhibiting the coexistence of first- and second-order phase transition properties.

ACKNOWLEDGMENT

This work was supported in part by the Converging Research Center Program through the Ministry of Science, ICT and Future Planning, Korea under Grant 2015055808, and was also supported in part by the Vietnam National Foundation for Science and Technology Development (NAFOSTED) under Grant 103.02-2014.17 (Quantum surface effects in low dimensional systems). A part of the work was done in the Key Laboratory for Electronic Materials and Devices, Institute of Materials Science, VAST, Vietnam.

REFERENCES

- Banerjee S K (1964), "On a generalised approach to first and second order magnetic transitions," *Phys. Lett.*, vol. 12, pp. 16–17, doi: [10.1016/0031-9163\(64\)91158-8](https://doi.org/10.1016/0031-9163(64)91158-8).
- Bonilla C M, Herreo-Albillos J, Bartolomé F, García L M, Parra-Borderías M, Franco V (2010), "Universal behavior for magnetic entropy change in magnetocaloric materials: An analysis on the nature of phase transitions," *Phys. Rev. B*, vol. 81, 224424, doi: [10.1103/PhysRevB.81.224424](https://doi.org/10.1103/PhysRevB.81.224424).
- Boutahar A, Phejar M, Paul Boncour V, Bessais L, Lassri H (2014), "Theoretical work in magnetocaloric effect of $\text{LaFe}_{13-x}\text{Si}_x$ compounds," *J. Supercond. Novel Magn.*, vol. 27, pp. 1795–1800, doi: [10.1007/s10948-014-2542-z](https://doi.org/10.1007/s10948-014-2542-z).
- Chandra S, Biswas A, Datta S, Ghosh B, Siriguri V, Raychaudhuri A K, Phan M H, Srikanth H (2012), "Evidence of a canted magnetic state in self-doped $\text{LaMnO}(3 + \delta)$ ($\delta = 0.04$): A magnetocaloric study," *J. Phys.: Condens. Matter*, vol. 24, 366004, doi: [10.1088/0953-8984/24/36/366004](https://doi.org/10.1088/0953-8984/24/36/366004).
- Chen X, Chen Y, Tang Y (2014), "Study of magnetocaloric effect in $\text{LaFe}_{11.5}\text{Si}_{1.5}$ alloys prepared by different cooling methods," *Bull. Mater. Sci.*, vol. 37, pp. 849–854, doi: [10.1007/s12034-014-0016-3](https://doi.org/10.1007/s12034-014-0016-3).
- Dubenko I, Khan M, Pathak A K, Gautam B R, Stadler S, Ali N (2009), "Magnetocaloric effects in Ni-Mn-X based Heusler alloys with X=Ga, Sb, In," *J. Magn. Mater.* vol. 321, pp. 754–757, doi: [10.1016/j.jmmm.2008.11.043](https://doi.org/10.1016/j.jmmm.2008.11.043).
- Franco V, Conde A (2010), "Scaling laws for the magnetocaloric effect in second order phase transitions: From physics to applications for the characterization of materials," *Int. J. Refrig.* vol. 33, pp. 465–473, doi: [10.1016/j.ijrefrig.2009.12.019](https://doi.org/10.1016/j.ijrefrig.2009.12.019).
- Franco V, Blázquez J S, Ingale B, Conde A (2012), "The magnetocaloric effect and magnetic refrigeration near room temperature: Materials and models," *Annu. Rev. Mater. Res.*, vol. 42, pp. 305–342, doi: [10.1146/annurev-matsci-062910-100356](https://doi.org/10.1146/annurev-matsci-062910-100356).
- Gschneidner K A, Pecharsky V K (2008), "Thirty years of near room temperature magnetic cooling: Where we are today and future prospects," *Int. J. Refrig.*, vol. 31, pp. 945–961, doi: [10.1016/j.ijrefrig.2008.01.004](https://doi.org/10.1016/j.ijrefrig.2008.01.004).
- Gschneidner K A, Pecharsky V K, Tsokol A O (2005), "Recent developments in magnetocaloric materials," *Rep. Prog. Phys.*, vol. 68, pp. 1479–1539, doi: [10.1088/0034-4885/68/6/R04](https://doi.org/10.1088/0034-4885/68/6/R04).
- Hu F-X, Shen B-G, Sun J-R, Cheng Z-H, Rao G-H, Zhang X-X (2001), "Influence of negative lattice expansion and metamagnetic transition on magnetic entropy change in the compound $\text{LaFe}_{11.4}\text{Si}_{1.6}$," *Appl. Phys. Lett.*, vol. 78, pp. 3675–3677, doi: [10.1063/1.1375836](https://doi.org/10.1063/1.1375836).
- Jia L, Sun J R, Shen J, Dong Q Y, Zou J D, Gao B, Zhao T Y, Zhang H W, Hu F X, Shen B G (2009), "Magnetocaloric effects in the $\text{La}(\text{Fe}, \text{Si})_{13}$ intermetallics doped by different elements," *J. Appl. Phys.*, vol. 105, 07A924, doi: [10.1063/1.3072021](https://doi.org/10.1063/1.3072021).
- Pathak A K, Khan M, Dubenko I, Stadler S, Ali N (2007), "Large magnetic entropy change in $\text{Ni}_{50}\text{Mn}_{50-x}\text{In}_x$ Heusler alloys," *Appl. Phys. Lett.*, vol. 90, 262504, doi: [10.1063/1.2752720](https://doi.org/10.1063/1.2752720).
- Pecharsky V K, Gschneidner K A (1997), "Giant magnetocaloric effect in $\text{Gd}_5(\text{Si}_2\text{Ge}_2)$," *Phys. Rev. Lett.*, vol. 78, pp. 4494–4497, doi: [10.1103/PhysRevLett.78.4494](https://doi.org/10.1103/PhysRevLett.78.4494).
- Phan M-H, Yu S-C (2007), "Review of the magnetocaloric effect in manganite materials," *J. Magn. Mater.*, vol. 308, pp. 325–340, doi: [10.1016/j.jmmm.2006.07.025](https://doi.org/10.1016/j.jmmm.2006.07.025).
- Provenzano V, Shapiro A J, Shull R D (2004), "Reduction of hysteresis losses in the magnetic refrigerant $\text{Gd}_5\text{Ge}_2\text{Si}_2$ by the addition of iron," *Nature*, vol. 429, pp. 853–857, doi: [10.1038/nature02657](https://doi.org/10.1038/nature02657).
- Tishin A M, Spichkin Y I (2003), *The Magnetocaloric Effect and its Applications*. Bristol, U.K.: IOP.
- Wang D, Han Z, Cao Q, Huang S, Zhang J, Du Y (2005), "The reduced Curie temperature and magnetic entropy changes in $\text{Gd}_{1-x}\text{In}_x$ alloys," *J. Alloys Comp.*, vol. 396, pp. 22–24, doi: [10.1016/j.jallcom.2004.12.004](https://doi.org/10.1016/j.jallcom.2004.12.004).
- Wood M E, Potter W H (1985), "General analysis of magnetic refrigeration and its optimization using a new concept: Maximization of refrigerant capacity," *Cryogenics*, vol. 25, pp. 667–683, doi: [10.1016/0011-2275\(85\)90187-0](https://doi.org/10.1016/0011-2275(85)90187-0).